JGR Oceans

RESEARCH ARTICLE
10.1029/2024JC022310

Special Collection:
Years of the Maritime Continent

Mooring-Observed Cross Equator Propagation of Kelvin Waves Through the Makassar Strait

Tengfei Xu[1,2], Shujiang Li[1,2], Yingyi Yang[1,2], Yaohua Zhu[1,2], A. Kuswardani[3], Yonggang Wang[1,2], Guanlin Wang[1,2], Xiaoqing Xu[1,2], Fei Teng[1,2], Agus Setiawan[4], Priyadi Dwi Santoso[5], Teguh Agustiadi[4], Mukti Trenggono[6], R. Dwi Susanto[7,8], and Zexun Wei[1,2]

[1]Key Laboratory of Marine Science and Numerical Modeling, First Institute of Oceanography, Ministry of Natural Resources of China, Qingdao, China, [2]Laboratory for Regional Oceanography and Numerical Modeling Qingdao Marine Science and Technology Center, Qingdao, China, [3]Agency for Marine and Fisheries Research and Human Resources, Ministry of Marine Affairs and Fisheries, Jakarta, Indonesia, [4]Research Center for Deep Sea, National Research and Innovation Agency, Jakarta, Indonesia, [5]Research Center for Oceanography, National Research and Innovation Agency, Jakarta, Indonesia, [6]Department of Marine Science, Faculty of Fisheries and Marine Science, Jenderal Soedirman University, Purwokerto, Indonesia, [7]Department of Atmospheric and Oceanic Science, University of Maryland, College Park, MD, USA, [8]Faculty of Earth Sciences and Technology, Bandung Institute of Technology, Bandung, Indonesia

Abstract The propagation of intraseasonal Kelvin waves in the Indonesian seas significantly modulates the Indonesian Throughflow (ITF) transport. However, their northward propagation across the equator within the main ITF route, particularly through the Makassar Strait, has remained unverified due to a lack of in situ observations. This study presents simultaneous mooring observations of current velocity profiles at the choke points in the ITF's main pathway, from the Lombok Strait to the northern Makassar Strait. Our results confirm the propagation of intraseasonal Kelvin waves cross the equator reaching the northern Makassar Strait, primarily along the 100-m isobath. During the propagation, the dominant modes are the first and second baroclinic modes in the Indian Ocean, the second and third baroclinic modes between the Lombok and southern Makassar Straits, and the third to fifth baroclinic modes between the southern and northern Makassar Straits. Vertical mode decomposition reveals that the intraseasonal velocity anomaly in the northern Makassar Strait comprises the first five baroclinic modes, with the first two modes dominant in the upper 400 m and the third to fifth modes dominant at depths of 400–800 m. Our finding establishes the Makassar Strait as a definite pathway for the cross-equator propagation of Kelvin waves, linking wave dynamics between the Pacific and Indian Oceans.

Plain Language Summary Previous research studies have indicated the propagation of intraseasonal Kelvin waves from the central equatorial Indian Ocean to the Lombok Strait, primarily in the first two baroclinic modes. Upon penetrating the Lombok Strait, these waves continue their northward journey along the 100-m isobath as the second and third baroclinic modes, reaching the southern Makassar Strait. This study, based on comprehensive mooring observations, provides evidence of these Kelvin waves sequentially crossing the equator and reaching the northern Makassar Strait, potentially continuing eastward along the north coast of Sulawesi Island. Notably, during their propagation, the dominant baroclinic modes undergo transformations: from the first and second modes in the Indian Ocean, to the second and third modes between Lombok and southern Makassar, and finally to the third to fifth modes across the Makassar Strait. The cross-equator propagation of Kelvin waves through the Makassar Strait plays a pivotal role in linking oceanic fluctuations between the Pacific and Indian Oceans.

Key Points:

- Indian Ocean Kelvin waves can penetrate into Indonesian seas via Lombok Strait and further northward cross equator through Makassar Strait
- First and second (third to fifth) baroclinic modes dominate the upper 400 m (400–800 m) in the northern Makassar Strait
- The increasing contribution of higher baroclinic mode Kelvin waves in the Indonesian seas could be due to significant stratification changes

Correspondence to:
Z. Wei,
weizx@fio.org.cn

Citation:
Xu, T., Li, S., Yang, Y., Zhu, Y., Kuswardani, A., Wang, Y., et al. (2025). Mooring-observed cross equator propagation of Kelvin waves through the Makassar Strait. *Journal of Geophysical Research: Oceans*, *130*, e2024JC022310. https://doi.org/10.1029/2024JC022310

Received 30 DEC 2024
Accepted 28 MAR 2025

Author Contributions:
Conceptualization: Tengfei Xu, Zexun Wei
Data curation: Tengfei Xu, Shujiang Li, Yingyi Yang
Formal analysis: Tengfei Xu, Shujiang Li, Yingyi Yang, Yaohua Zhu
Funding acquisition: Zexun Wei
Investigation: Tengfei Xu, Shujiang Li, A. Kuswardani, Guanlin Wang, Xiaoqing Xu, Fei Teng, Agus Setiawan, Priyadi Dwi Santoso, Teguh Agustiadi, Mukti Trenggono
Methodology: Tengfei Xu
Project administration: Yonggang Wang
Resources: Tengfei Xu
Supervision: Zexun Wei
Validation: Tengfei Xu, Shujiang Li, Yaohua Zhu
Visualization: Yingyi Yang
Writing – original draft: Tengfei Xu, Zexun Wei

1. Introduction

The Indonesian seas, situated between the Pacific and Indian Oceans, provide the only tropical pathway for inter-ocean water exchange in the global circulation (Gordon & Fine, 1996; Wyrtki, 1961). This pathway, known as the Indonesian Throughflow (ITF), carries approximately 15 Sv (1 Sv = 10^6 m^3 s^{-1}) of volume and 0.5–1 PW (1 PW = 10^{15} W) of heat flux from Pacific Ocean to the Indian Ocean (Gordon et al., 2010; Li et al., 2018; Sprintall et al., 2009; Tillinger & Gordon, 2010; Xie et al., 2019; Xu et al., 2024; Zhang et al., 2019). Consequently, the ITF plays a crucial role in maintaining the heat and salt balances of the tropical Indian and Pacific Oceans (Sprintall et al., 2014), and even contributes significantly to the global thermohaline circulation by

Writing – review & editing: Tengfei Xu, Shujiang Li, Yingyi Yang, Yaohua Zhu, A. Kuswardani, Yonggang Wang, Guanlin Wang, Xiaoqing Xu, Fei Teng, Agus Setiawan, Priyadi Dwi Santoso, R. Dwi Susanto, Zexun Wei

funneling more than half of the waters from the Indian Ocean to the Atlantic Ocean via the Agulhas channel, ultimately feeding the North Atlantic Deep Water (NADW) (Durgadoo et al., 2017; Gordon, 1986).

The ITF region serves as the nexus of two distant equatorial waveguides: Rossby waves from the Pacific and Kelvin waves from the Indian Ocean (Wijffels & Meyers, 2004). Intraseasonal Kelvin waves have been identified along the south coast of the Sumatra–Java Islands using tide gauge and satellite sea level data (Arief & Murray, 1996; Horii et al., 2016; Iskandar et al., 2005; Xu et al., 2016), as well as mooring-measured current velocity data (Gordon et al., 2010; Pujiana et al., 2009, 2012, 2013; Sprintall et al., 2009). These intraseasonal Kelvin waves originate in the central equatorial Indian Ocean, where wind anomalies trigger their generation and subsequent eastward propagation along the equator to the south coast of the Sumatra–Java Islands (Chen et al., 2015, 2016; Schiller et al., 2010). Upon reaching the straits along the island chain, part of the Kelvin wave energy can penetrate and induce significant intraseasonal variability in sea level and horizontal currents, such as in the Sunda, Lombok, Ombai, and Savu Straits (Drushka et al., 2010; Iskandar et al., 2014; Li et al., 2018; Wang et al., 2020; Xu et al., 2018). The branch that traverses the Lombok Strait continues northward along the 100-m isobath to reach the southern mouth of the Makassar Strait, potentially reducing the southward ITF in the Makassar Strait by up to 2 Sv (Pujiana et al., 2013). The Makassar Strait is the primary inflow pathway for the ITF, with a water transport of approximately 12.5 Sv, representing around 77% of the total ITF that conveys Pacific water to the Indian Ocean across the Indonesian seas (Gordon et al., 2019). Therefore, the propagation of intraseasonal Kelvin waves plays a pivotal role in modulating the ITF transport.

Recent studies by Pujiana and McPhaden (2020) investigated the structure and propagation of intraseasonal Kelvin waves from the central equatorial Indian Ocean to the Indonesian seas using moored velocity time series. Their findings align with previous studies regarding the Kelvin wave pathways and highlight the dominance of the second baroclinic mode Kelvin wave. Additionally, there is evidence of the third and fourth baroclinic mode Kelvin waves traveling from the Lombok Strait to the Makassar Strait. Linear reduced-gravity ocean models have demonstrated the Kelvin waves' ability to propagate through the Makassar Strait into the Pacific Ocean, inducing interannual variability in the Maluku Channel (Terada & Masumoto, 2023; Yuan et al., 2018). Kelvin wave signals have also been detected by moored current velocity measurements in the Maluku Channel, exhibiting characteristics derived from both the Indian and Pacific Oceans (Hu et al., 2019, 2022). However, due to the lack of direct observations in the northern Makassar Strait, it remains unclear whether and how the Kelvin waves traverse the Makassar Strait across the equator.

As part of the China–Indonesia collaboration under the Indonesia-China Center for Ocean and Climate (ICCOC), an international cooperation project titled "The Transport, Internal Waves and Mixing in the Indonesian Throughflow regions (TIMIT) and Impacts on Marine Ecosystem" was jointly proposed by the First Institute of Oceanography (FIO) of the Ministry of Natural Resources of China and the Agency for Marine & Fisheries Research (AMFR) of the Ministry of Marine Affairs and Fisheries of Indonesia in December 2013. TIMIT cruises deployed subsurface moorings in the Lombok Strait (8°25.14′S, 115°57.59′E) and the northern mouth of the Makassar Strait (0°57.09′N, 119°15.95′E), capturing current velocity time series from 20 October 2015 to 22 September 2016. These observations overlap with the mooring data used in Pujiana and McPhaden (2020) from the southern mouth of the Makassar Strait. The TIMIT observations provide an opportunity to unravel the propagation of Indian Ocean Kelvin waves through the Makassar Strait, which is the focus of this study. The remainder of this paper is organized as follows: Section 2 describes the data and methods used; Section 3 presents the Kelvin wave structure and propagation in the Makassar Strait; Section 4 discusses the findings and draws conclusions; and Section 5 provides a summary.

2. Data and Methods

2.1. Field Measurements

In this study, time series of mooring-observed current profiles in the equatorial Indian Ocean, the Lombok and Makassar Straits were used to track the pathway of the intraseasonal Kelvin waves in the Makassar Strait. As part of the Research Moored Array for African-Asian-Australian Monsoon Analysis and Prediction (RAMA), there are two subsurface moorings at 80.5°E (EQW) and 90°E (EQE) in the equatorial Indian Ocean, which have recorded the velocity profiles since October 2004 and November 2000, respectively (McPhaden et al., 2009, 2015). The subsurface mooring in the southern part of the Makassar Strait (MakS: 2°51.9′S, 118°27.3′E) is provided by the Monitoring the ITF (MITF) project (Gordon et al., 2019). The subsurface moorings in the

Lombok and northern part of the Makassar Straits were supported by the TIMIT project, deployed at stations Lom (8°25.14′S, 115°57.59′E) and MakN (0°57.09′N, 119°15.95′E), respectively (Wei et al., 2019). For consistency, we use the overlap period of the RAMA, MITF, and TIMIT moorings, that is, from 2015.10.20 to 2016.09.22. These mooring-observed zonal (u) and meridional (v) components of the currents were interpolated with vertical depth interval of 10 m. In addition, the TIMIT project has carried out 44 CTD casts along the main route of the ITF. The World Ocean Atlas 2018 (WOA18) has provided gridded hydrographic data in the study area. The temperature and salinity obtained from both TIMIT and WOA18 were used for the calculation of stratification and vertical mode decomposition.

2.2. Satellite and Reanalysis Products

The daily sea level anomaly (SLA) was obtained from Copernicus Marine Environment Monitoring Service (CMEMS) and can be downloaded at https://doi.org/10.48670/moi-00148. The dataset ID is SEALEVEL_GLO_PHY_L4_MY_008_047, with a horizontal resolution of 0.25° × 0.25°. The European Center for Medium-Range Weather Forecasts (ECMWF) released the ERA5 global reanalysis, providing hourly wind fields on a 0.25° × 0.25° gird point, and it was used to force the Kelvin wave model.

2.3. Kelvin Wave Identification

To capture the phase propagation and vertical structure of the intraseasonal Kelvin waves, the complex empirical orthogonal function (CEOF) method was applied to SLAs and mooring-observed horizontal currents, respectively, following calculations similar to those in Iskandar and McPhaden (2011) and Pujiana and McPhaden (2020).

2.4. Vertical Mode Decomposition

The vertical structures of the Kelvin waves are investigated by decomposing them into different baroclinic modes (Drushka et al., 2010; Iskandar et al., 2006). Following Gill (1982), the governing equations can be solved using the modal decomposition method. The nth mode baroclinic Kelvin wave, which is represented by the vertical eigenfunction ψ_n, can be written as follows:

$$\frac{\partial y}{\partial x}\left[\frac{1}{N(z)^2}\frac{\partial \psi_n(z)}{\partial z}\right] = \frac{1}{c_n^2}\psi_n(z)$$

with the boundary conditions

$$\frac{\partial \psi_n(0)}{\partial z} = \frac{\partial \psi_n(H)}{\partial z} = 0$$

and normalized such that

$$\int_{-H}^{0} \psi_n^2(z)\, dz = H$$

where $N(z)$ is the Brunt–Väisälä frequency, H is the bottom depth, and c_n is the phase speed of the nth mode baroclinic Kelvin wave.

2.5. Wind Forcing Model

A wind forcing model was employed to examine the Kelvin wave dynamics along its waveguide (Drushka et al., 2010). Considering the ocean as linear and continuously stratified, the Kelvin wave is then determined by integrating the wind stress along the characteristic $x–ct = constant$, from the central equatorial Indian Ocean to a point x_0 along the waveguide. Each mode of the Kelvin waves A_n is calculated individually as follows:

$$A_n(x_0, z, t) = \alpha_n(z)\int_{70°\mathrm{E}}^{x_0} \tau^x\left(x, t + \frac{x - x_0}{c_n}\right) dx$$

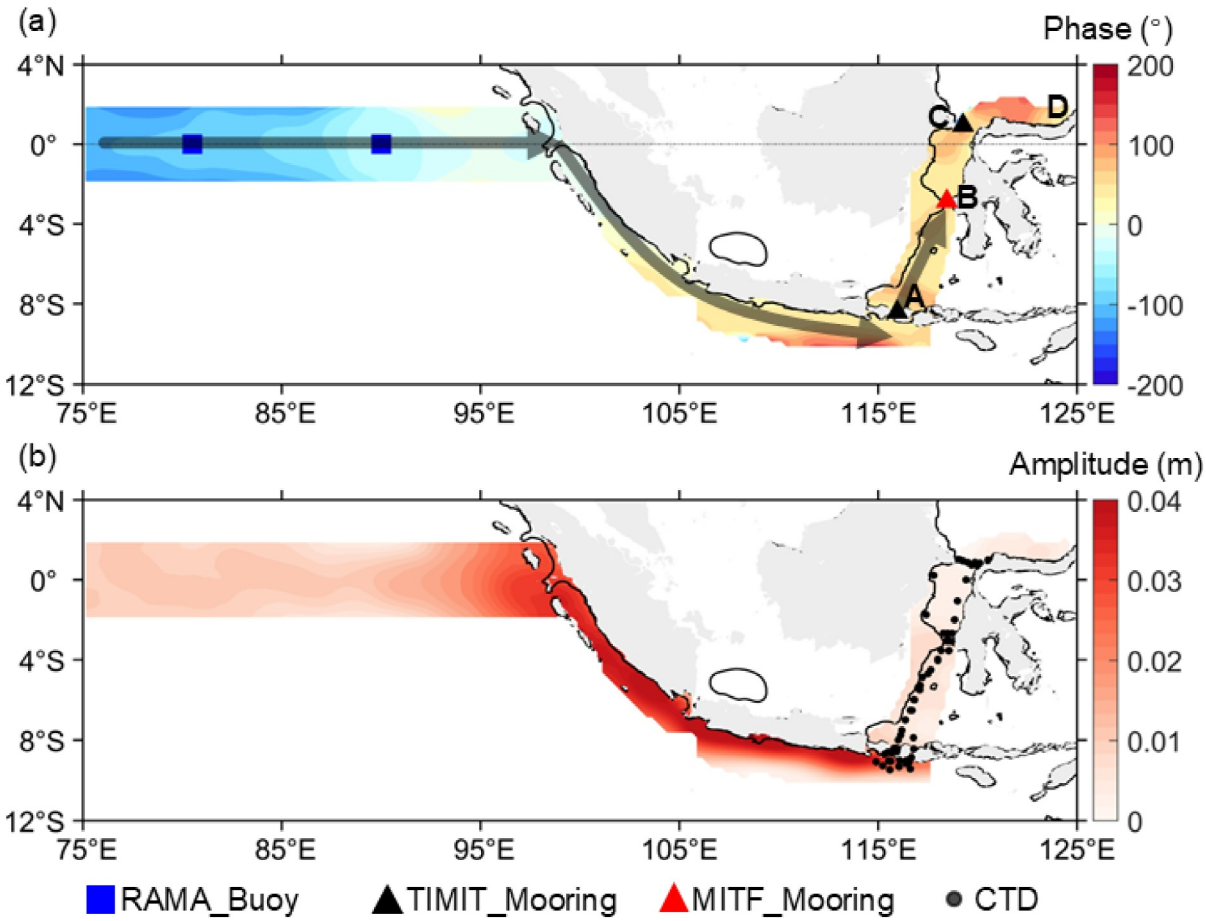

Figure 1. Mooring and CTD sites along the pathway of the intraseasonal Kelvin waves. (a) Phase and (b) amplitude of the first mode of the complex empirical orthogonal function (CEOF) for intraseasonal sea level anomaly (SLA) with a bandpass filter of 20–90 days. Arrows in (a) indicate the pathway of the intraseasonal Kelvin waves; black contours are the 100-m isobath; the letters A, B, C, and D denote the chokepoints along the waveguide, that is, the Lombok Strait, southern Makassar Strait, northern Makassar Strait, and Manado coast, respectively. Note A, B, and C are located at the mooring sites Lom (8°25.14′S, 115°57.59′E), MakS (2°51.9′S, 118°27.3′E), and MakN (0°57.09′N, 119°15.95′E).

where A_n represents the SLA or current velocity of the nth mode Kelvin wave and α_n is the corresponding signal coefficient; τ^x is the wind stress along the waveguide as shown in Figure 1. The sum of A_n yields the total Kelvin wave response to the wind force. For A_n referred to as the SLA, $\alpha_n = \psi_n(0)^2/\rho g H$; for A_n referred to as the current velocity, $\alpha_n = \psi_n(0)\,\psi_n(z)/\rho c_n H$ (Kessler et al., 1995). Table 1 gives the values of α_n and c_n adopted in this study.

2.6. Volume Transport Calculation

First, we interpolated the v-component of MakN mooring observation across the transect (0°57.09′N, 118°58.88′–120°14.63′) with no-slip boundary condition. Then, the transport is estimated by integrating the v-component in the transect as follows:

$$F_V = \sum_{k=1}^{k=n}\left[\Delta z_k \sum_{i=1}^{i=m} \Delta l_i v_{i,k}\right]$$

where $v_{i,k}$ is the averaged v-component velocity across the transect within the grid box of Δz_k (thickness) by Δl_i (width)., and topography extracted from the General Bathymetric Chart of the Oceans (GEBCO). GEBCO provides global bathymetric and topographic data at 15 arc-second grid resolution (~450 m), which can be downloaded from https://www.gebco.net/data_and_products/gridded_bathymetry_data/gebco_2022/.

Table 1
The Mean Theoretical Kelvin Wave Phase Speeds c_n, Signal Coefficients α_n, and Estimated Travel Time for Each Kelvin Wave Mode Along Its Waveguide

				Lom–MakS (days)		MakS–MakN (days)	
n	c_n (m/s)	α_n/SLA ($\times 10^{-8}$)	α_n/velocity ($\times 10^{-7}$)	Real	Theory	Real	Theory
1	2.41 ± 1.02	4.96	1.74	10–16	6	8–12	3
2	1.20 ± 0.51	3.46	2.84		12		6
3	0.80 ± 0.34	3.04	3.65		18		9
4	0.60 ± 0.25	4.32	4.61		24		13
5	0.48 ± 0.20	5.96	5.50		30		15

Note. The mean and standard deviation values of c_n are calculated based on the range of stratifications observed in the equatorial Indian Ocean and Lombok and Makassar Straits.

3. Results

3.1. Propagation of the Intraseasonal Kelvin Waves Observed by Satellite Altimetry

The intraseasonal Kelvin wave pathways in the Indian Ocean and Indonesian seas were examined by using satellite altimetry data and employing techniques such as snapshot analysis, lag correlation, and CEOF decomposition of intraseasonal sea level anomaly (SLA) (Pujiana et al., 2013; Pujiana & McPhaden, 2020; Xu et al., 2016). Herein, we focused on CEOF analysis of bandpass-filtered SLA data, with period cut-offs of 20–90 days, along the Kelvin wave propagation pathway. The first CEOF mode accounted for 61% of the total variance, highlighting its dominance (Figure 1).

The phase progression of the first CEOF mode indicates Kelvin wave propagation from the central equatorial Indian Ocean eastward, continuing southeastward along the Sumatra–Java coast, and then northeastward upon entering the Lombok Strait (Figure 1a). This phase evolution suggests Kelvin waves' capability to traverse the equator and reach the north coast of Manado (Point D in Figure 1a). Along the Sumatra–Java coast, the Kelvin wave amplitudes amplify, followed by attenuation after they enter Indonesian waters via the Lombok Strait. Specifically, the intraseasonal amplitudes in the Makassar Strait and along the north coast of Sulawesi are approximately 0.01 m, representing roughly 25% of those observed along the Sumatra–Java coast (Figure 1b).

To further validate the Kelvin wave propagation, Hovmöller diagrams along the waveguide were constructed from both reconstructed and predicted intraseasonal SLA data (Figure 2). These diagrams consistently reveal Kelvin wave propagation from the central equatorial Indian Ocean to the Sulawesi Sea. During the observational period from October 2015 to September 2016, a total of 8 upwelling and 8 downwelling Kelvin wave events were identified. These events were triggered by intraseasonal easterly and westerly wind anomalies in the central equatorial Indian Ocean, respectively. These findings collectively demonstrated the coherent propagation and variability of intraseasonal Kelvin waves across the Indian Ocean and Indonesian seas, as detected and analyzed using satellite altimetry techniques.

3.2. Intraseasonal Variability Observed in Mooring Velocities

Intraseasonal signals were robustly detected in current velocities observed by moorings deployed in the central equatorial Indian Ocean and the Lombok and Makassar Straits (Figure 3). During the observational period from October 2015 to September 2016, significant eastward flows occurred in December 2015, February, March, May, June, July, and from August–September 2016, with maximum velocity anomalies reaching up to 0.55 m/s in the central equatorial Indian Ocean (Figures 3a and 3b). These intraseasonal velocity anomalies propagated eastward as equatorial Kelvin waves, reaching the eastern boundary of the Indian Ocean. Upon reaching the Sumatra–Java coast, they transitioned into coastal Kelvin waves, which continued along the coastline. As these waves arrived at the Lombok Strait, they penetrated into the Indonesian seas and traveled further northward, inducing intraseasonal variability in current velocities in the Lombok and Makassar Straits. The intraseasonal Kelvin waves were evident from the upward phase propagation in the bandpass-filtered velocity profiles and the timing lags of several days to months compared to the central equatorial Indian Ocean (Figures 3c–3e).

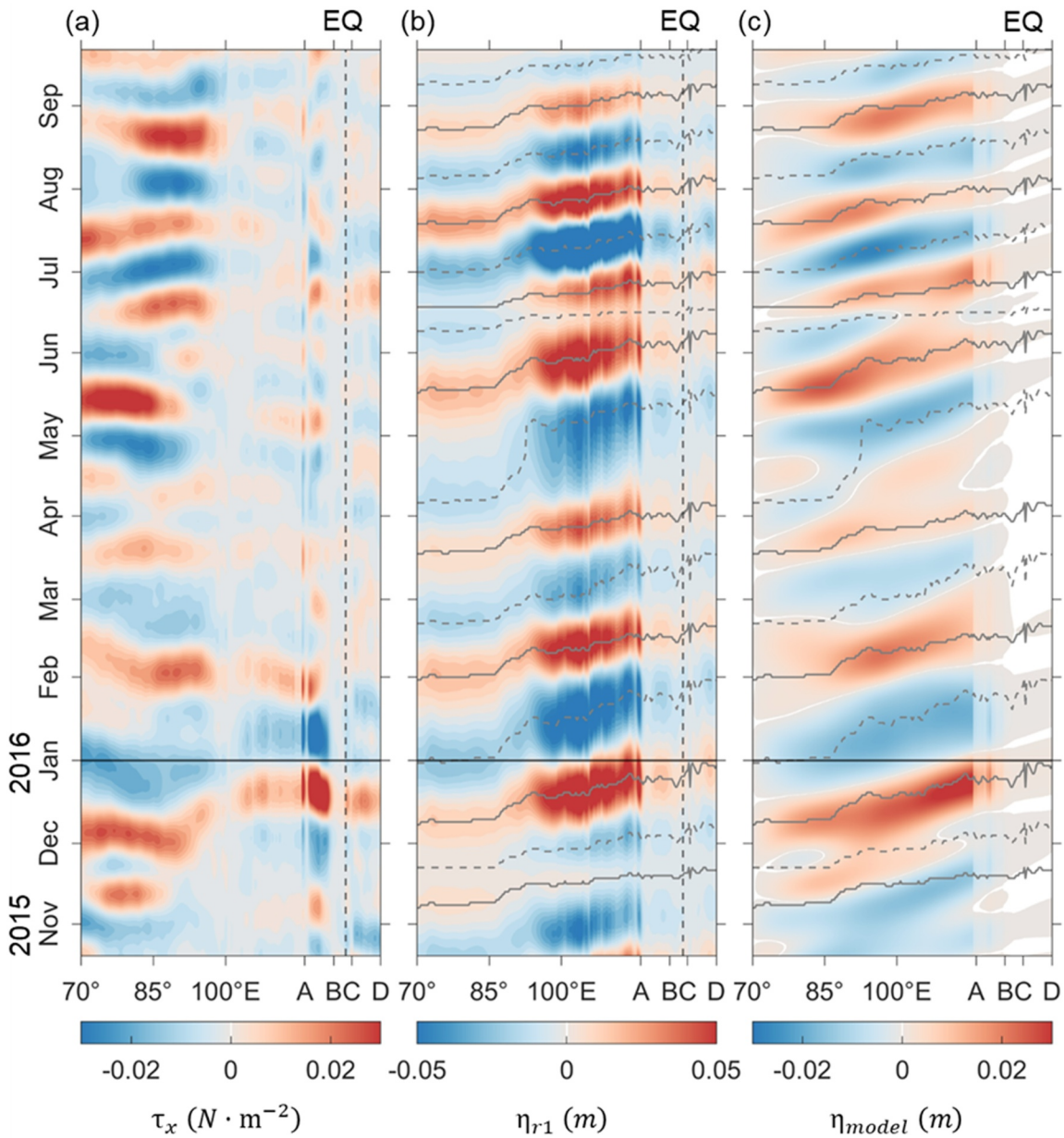

Figure 2. Hovmöller diagrams along the pathway of the Kelvin waves. (a) Intraseasonal zonal wind stress (τ_x), (b) reconstructed intraseasonal SLA (η_{r1}) based on the first mode of CEOF, and (c) predicted intraseasonal SLA (η_{model}) based on the wind forcing model. Solid (dashed) lines denote the upwelling (downwelling) Kelvin waves. The letters A, B, C, and D denote the chokepoints along the waveguide, that is, the Lombok Strait, southern Makassar Strait, northern Makassar Strait, and Manado coast, respectively, as marked in Figure 1a.

The first CEOF modes were used to reconstruct velocity anomalies at the mooring sites (Figure 4). These modes accounted for 78.20% and 81.43% of the variance at 80.5°E (EQW) and 90°E (EQE) at the equator, respectively, and 71.14%, 57.27%, and 62.58% in the Lombok, southern, and northern Makassar Straits, respectively. The reconstructed velocity anomalies at EQW and EQE exhibited intraseasonal variability with vertically upward phase shifts, indicating the propagation of intraseasonal Kelvin waves. Notably, the intraseasonal signals at 90°E lagged those at 80.5°E by several days, corresponding to a phase speed range of 1.55–2.63 m/s, which was consistent with previous studies (Iskandar & McPhaden, 2011; Pujiana & McPhaden, 2020).

The identified intraseasonal signals were equatorial Kelvin waves that propagated eastward and transitioned into coastally trapped Kelvin waves upon reaching the Sumatra coast (Iskandar et al., 2005; Iskandar &

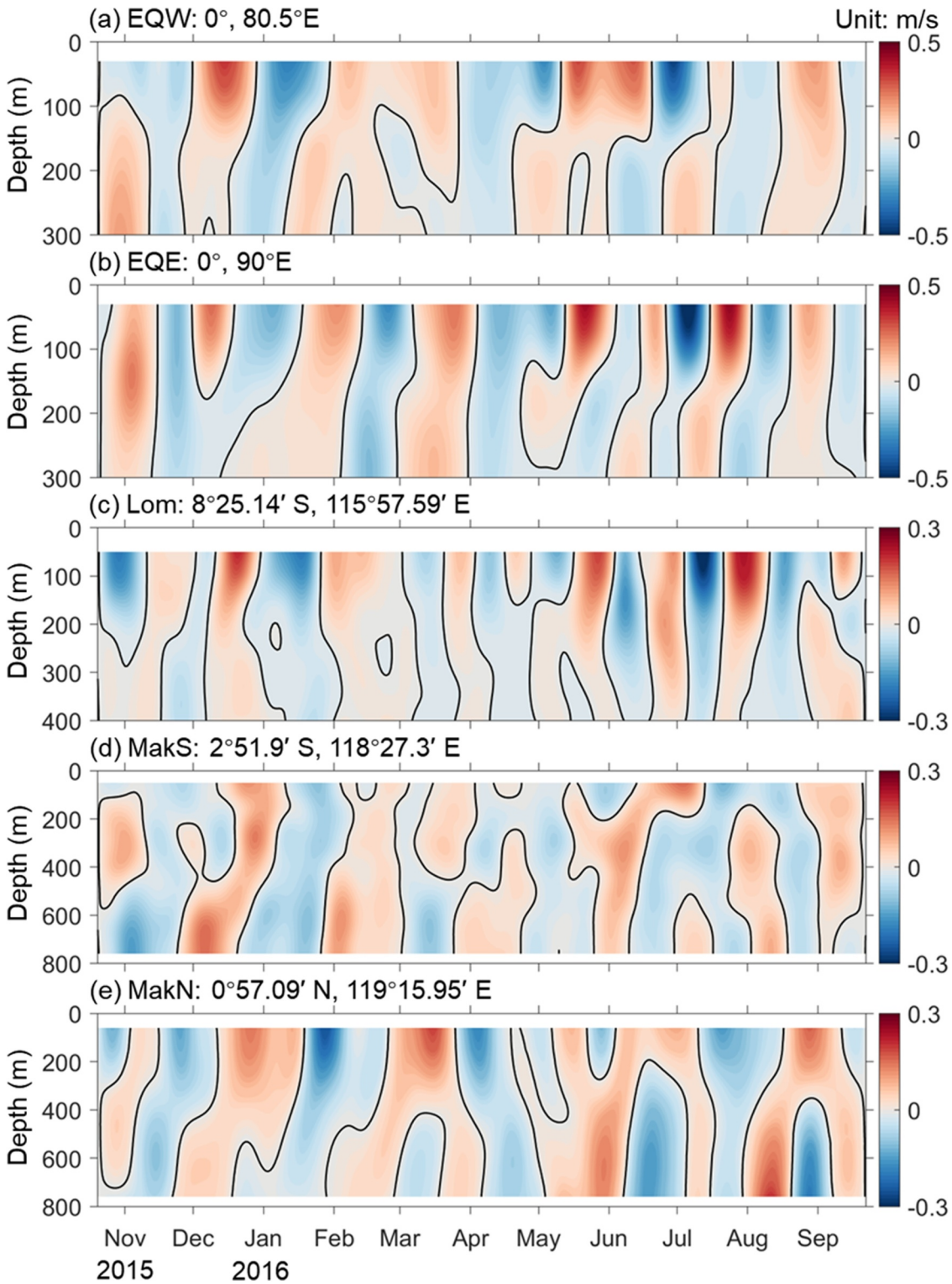

Figure 3. Bandpass filtered current velocity with cut-off period of 20–90 days. (a) Zonal velocity at EQW (0°, 80.5°E) and (b) EQE (0°, 90°E); and along-strait velocity in (c) Lombok Strait (Lom: 8°25.14′S, 115°57.59′E), (d) southern Makassar Strait (MakS: 2°51.9′S, 118°27.3′E) and (e) northern Makassar Strait (MakN: 0°57.09′N, 119°15.95′E).

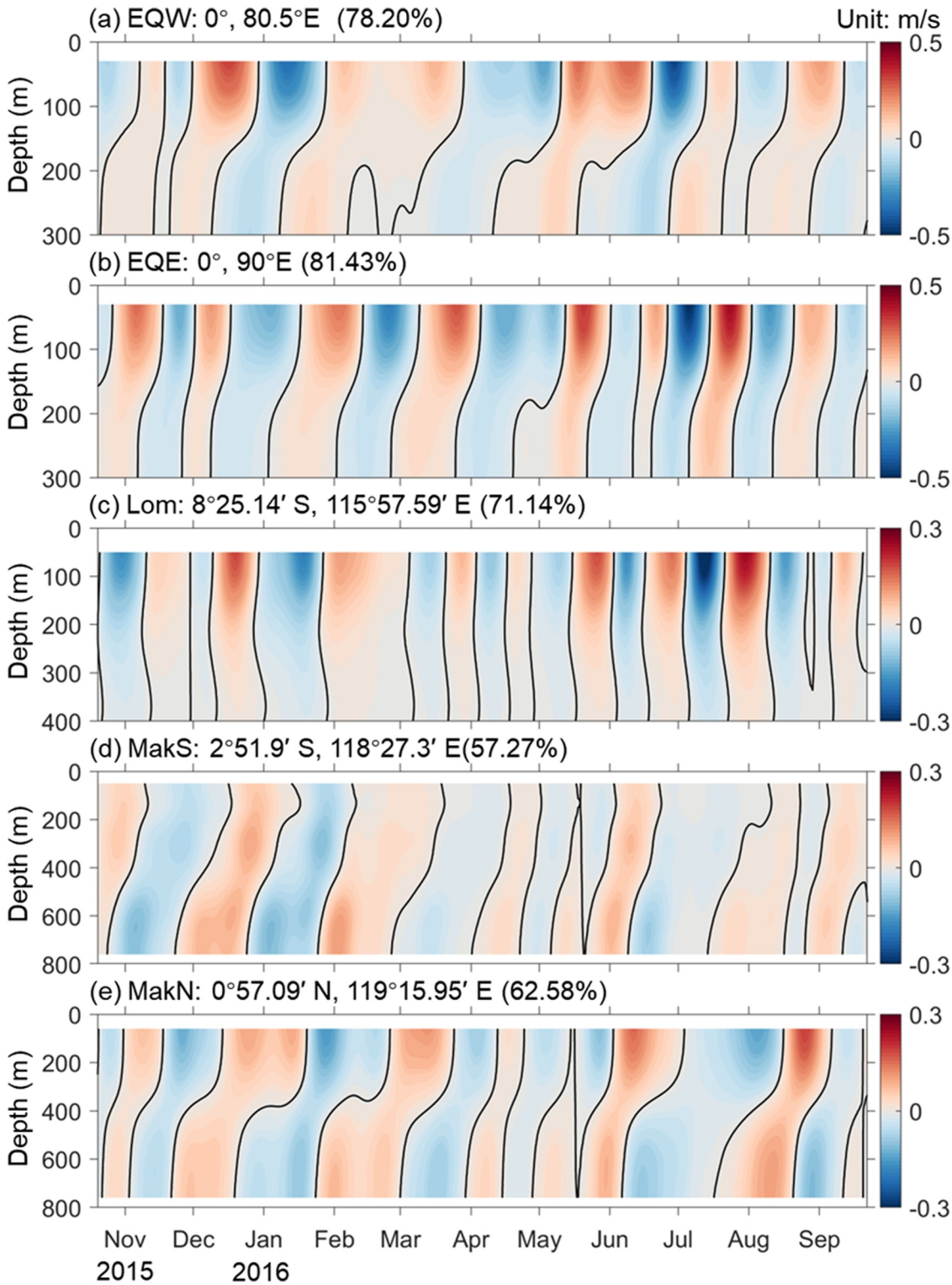

Figure 4. Reconstructed intraseasonal current velocity anomaly based on the first CEOF mode. (a) Zonal velocity at EQW (0°, 80.5°E) and (b) EQE (0°, 90°E); and along-strait velocity in (c) Lombok Strait (Lom: 8°25.14′S, 115°57.59′E), (d) southern Makassar Strait (MakS: 2°51.9′S, 118°27.3′E) and (e) northern Makassar Strait (MakN: 0°57.09′N, 119°15.95′E). The percentage numbers indicate the variance contribution of the first CEOF mode.

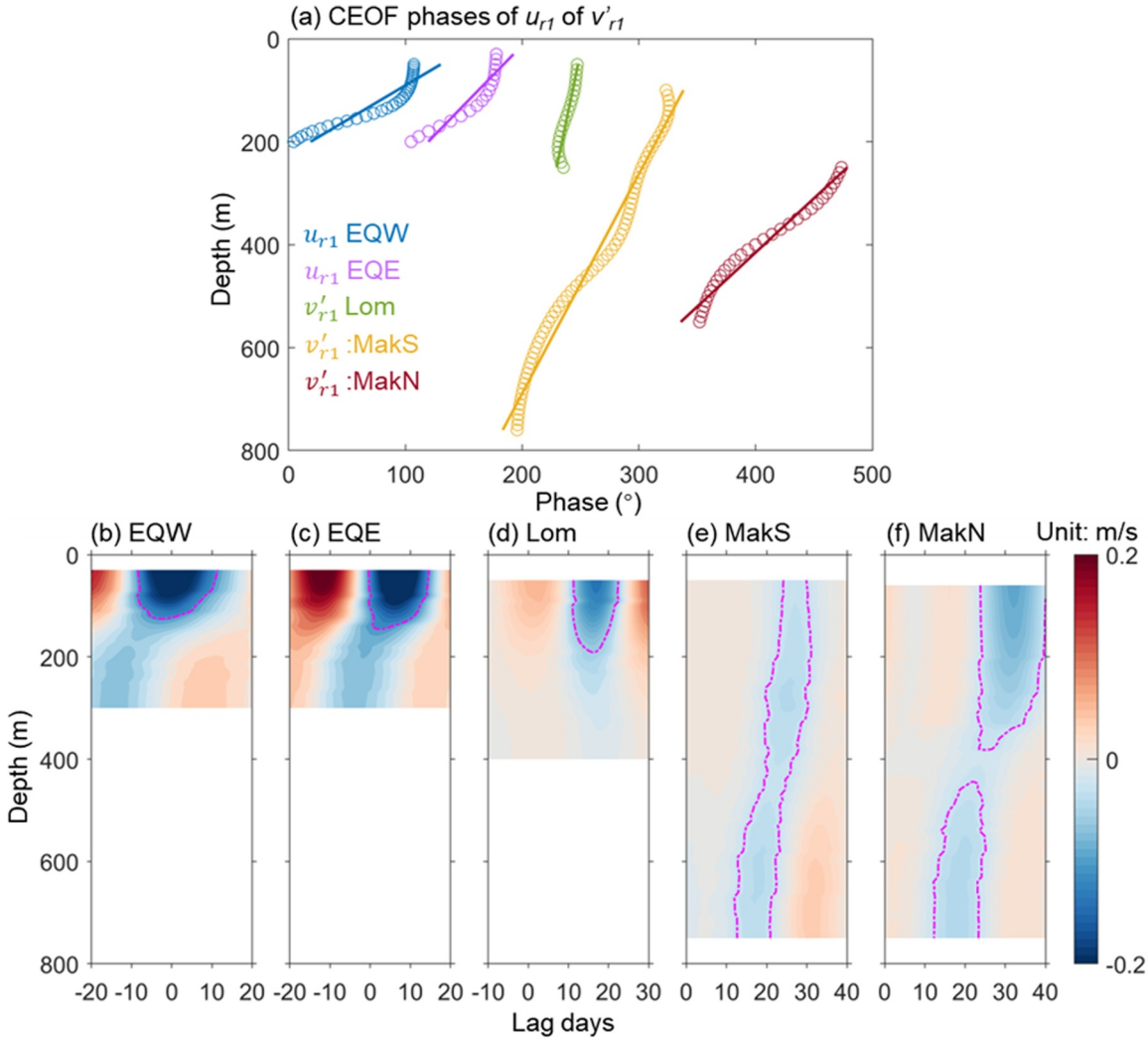

Figure 5. (a) CEOF phases of zonal velocity (u_{r1}) at EQW (0°, 80.5°E) and EQE (0°, 90°E), and along-strait velocity (v'_{r1}) in the Lombok Strait (Lom: 8°25.14′S, 115° 57.59′E), Makassar Strait South (MakS: 2°51.9′S, 118°27.3′E) and North (MakN: 0°57.09′N, 119°15.95′E). (b) Composites of u_{r1} and v'_{r1} induced by Kelvin waves at each mooring site during the observation period of 2015.10.20 to 2016.09.22. The phase in (a) at each mooring site is referenced to that at EQW at 100 m, with colored lines showing the linear least-squares fits to the CEOF phases. Dashed contours mark $u_{r1} = -0.1$ m s^{-1} in (b, c), $v'_{r1} = -0.05$ m s^{-1} in (d, e), and $v'_{r1} = -0.025$ m s^{-1} in (f).

McPhaden, 2011; Pujiana & McPhaden, 2020; Qiu et al., 1999; Schiller et al., 2010). These coastally trapped Kelvin waves propagated along the Sumatra–Java coast and were capable of penetrating the Lombok Strait, continuing northward to reach the Makassar Strait (Drushka et al., 2010; Iskandar et al., 2014; Pujiana et al., 2013). The intraseasonal variability in current velocities in the Lombok and Makassar Straits are shown in Figures 4c–4e. Notably, the velocity profiles in the Lombok Strait exhibited less upward tilt, suggesting a faster upward phase speed of the Kelvin waves compared to that of the equatorial Indian Ocean (Figure 4c). This may be partly attributed to weakened background stratification induced by strong tidal mixing in the Lombok Strait (Pujiana & McPhaden, 2020; Susanto et al., 2024).

The reconstructed velocity anomalies in Figures 4c–4e are similar to those reported by Pujiana and McPhaden (2020) in their Figure 3. Our mooring observations showed similar patterns of reconstructed velocity anomalies in the northern Makassar Strait compared to the southern Makassar Strait, with a time lag of a few days, indicating further northward propagation of the Kelvin waves (Figures 4d and 4e). In the following sections, we will further examine the signatures of these intraseasonal Kelvin waves and their propagation to the northern Makassar Strait.

3.3. Signature and Propagation of Intraseasonal Kelvin Waves

The CEOF phases of u_{r1} and v'_{r1} show upward propagation, with speeds roughly equivalent to 22 m day^{-1} (EQW), 23 m day^{-1} (EQE), 56 m day^{-1} (Lombok), 52 m day^{-1} (MakS), and 37 m day^{-1} (MakN) at period band of 20–90 days, respectively (Figure 5a). According to the linear ray theory, Kelvin wave propagates eastward (x) and downward (z) at an angle $\theta = \frac{dz}{dx} = -\frac{\omega}{N(z)}$, where ω is the frequency of the wind forcing (Drushka et al., 2010; McCreary & Anderson, 1984). In the depth (z)–time (t) coordinate, it can be written as $\theta = \frac{dz}{dx} = \frac{dz}{dt}\frac{dt}{dx} = -\frac{\omega}{N(z)}$, and thus $\frac{dz}{dt} = -\frac{\omega c}{N(z)}$, where $c = \frac{dx}{dt}$ is the horizontal speed of Kelvin wave. Consequently, the upward phase speeds in the equatorial Indian Ocean and the Indonesian straits can be estimated by the given ω at the period band of 20–90 days; c = 0.48–2.41 m s^{-1}; and N = 0.005734 s^{-1} (equatorial Indian Ocean), 0.009379 s^{-1} (Lombok Strait), and 0.009574 s^{-1} (Makassar Strait) derived from WOA 2018 and TIMIT CTD casts. The estimated values are 23 m day^{-1} (equatorial Indian Ocean), 40 m day^{-1} (Lombok Strait), and 39 m day^{-1} (Makassar Strait), which are in agreement with those from CEOF of observed velocity.

Figures 5b–5f show the composite of u_{r1} and v'_{r1} at each mooring sites, with day = 0 referring to as the peak of upwelling Kelvin waves at EQW. The results suggest lagging times of approximately 7 (EQE), 17 (Lombok), 27 (MakS), and 32 (MakN) days, respectively. This implies propagating speeds of 1.93 m s^{-1} (from EQW to EQE), 2.21 m s^{-1} (from EQE to Lombok), 0.50 m s^{-1} (from Lombok to MakS), and 0.52 m s^{-1} (from MakS to MakN). In comparison, the phase speed of equatorial Kelvin waves was estimated at values of 1.5–2.9 m s^{-1} along the southern coast of Sumatra and Java, and 0.8–1.3 m s^{-1} from Lombok to MakS, based on satellite altimetry and/or in situ observations (Iskandar et al., 2005; Pujiana & McPhaden, 2020; Pujiana et al., 2013; Syamsudin et al., 2004; Xu et al., 2016). Following McCreary and Anderson (1984), the theoretical phase speeds for the first five baroclinic modes are 2.41, 1.20, 0.80, 0.60, and 0.48 m s^{-1}, respectively (Table 1). Therefore, in addition to previously identified domination of mode 1 and mode 2 before entering the Indonesian seas, and mode 2 and mode 3 from the Lombok to MakS, we speculate that higher modes of Kelvin waves, that is, mode 4 and mode 5, also contribute to the intraseasonal velocity anomalies in the Makassar Strait.

The Kelvin wave signature is further revealed by the relation of wave frequency (ω) versus horizontal wavenumber (l) based on coherence analysis of the reconstructed velocities (Figure 6). The horizontal wavenumber in Figure 6a shows positive values, suggesting northward propagation from the Lombok Strait to MakS. Moreover, the observed distribution of ω–l generally falls in the theoretical dispersion curves between the second and fifth baroclinic Kelvin wave modes. The horizontal phase speed derived from the ω–l distribution gives a range of 0.51–2.57 m s^{-1}, which is in agreement with the theoretical phase speeds of the first five baroclinic modes of Kelvin waves (Table 1). For the vertical propagation of the coastal Kelvin wave in the Indonesian seas, the dispersion relation of ω with vertical wavenumber (m) can be represented as $\omega = \frac{N}{|m|}l$ (Romea & Allen, 1983). The vertically averaged Buoyancy frequency (N) in the upper 800 m is 0.0096 s^{-1} calculated from the TIMIT CTD data. Then, the m–l scatter of the Kelvin waves from Lombok to MakS can be derived, showing oscillation at intraseasonal frequencies with periods of 20–90 days (Figure 6b). Similarly, the dispersion diagrams of ω–l and m–l from MakS to MakN are shown in Figures 6c and 6d. Most of the scatters with $l > 0$ fall in the range of the third to fifth baroclinic Kelvin wave modes, with periods of 20–50 days (Figures 6c and 6d). In addition to the northward propagating mode 3 to mode 5 Kelvin waves from MakS to MakN, there are also southward propagating signals from MakN to MakS (Figure 5c). These southward propagating signals may be attributed to Rossby waves, albeit the ω–l scatters with $l < 0$ do not totally fit the theoretical dispersion curves of low frequency Rossby waves (Figure 5c).

3.4. Vertical Mode Decomposition and Wind Driven Model

In this section, we present the results of our vertical mode decomposition analysis and the application of a simple wind-driven model to elucidate the Kelvin wave dynamics in the northern Makassar Strait.

Vertical mode decomposition revealed the structures of the first five vertical modes based on the stratification in the Makassar Strait (Figure 7a). Mode 1 exhibits a positive structure in the upper 800 m, whereas modes 2 and 3 have one zero-crossing point at approximately 450 and 300 m, respectively. Modes 4 and 5 feature two zero-crossing points at around 180 and 650 m, and 140 and 490 m, respectively (Figure 7b). Among these, the first two baroclinic modes dominate the upper 200 m, representing averaged contributions of 24.25% (mode 1) and 28.81% (mode 2); mode 1 dominates 200–400 m, representing an averaged contribution of 58.11%; modes 3–5

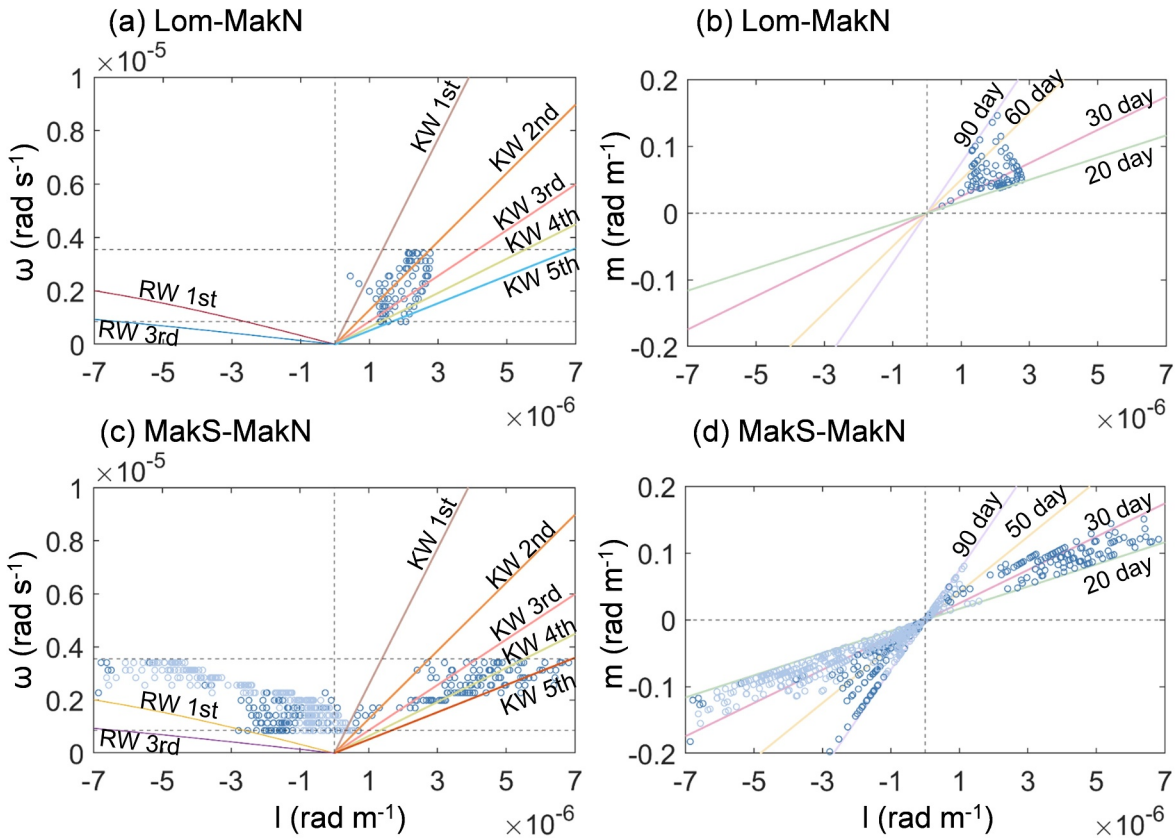

Figure 6. Dispersion diagrams of (a) wave frequency (ω) versus horizontal wavenumber (l), and (b) the vertical wavenumber (m) versus l inferred from coherence analyses of the reconstructed intraseasonal along-strait velocities in the Lombok and southern Makassar Straits. (c, d) are same as (a, b), but for those in the southern and northern Makassar Strait. Circles indicate the observed dispersion estimates, colored lines in (a, c) indicate the first five baroclinic Kelvin wave and first and third baroclinic Rossby wave dispersion curves; horizontal dashed black lines in (a, c) indicate the intraseasonal frequency band. Colored lines in (b, d) indicate the theoretical dispersion curves of the Kelvin waves for four different intraseasonal frequencies. The theoretical phase speeds of Kelvin waves are estimated based on buoyancy frequencies in WOA18 averaged within 114°–120°E, 2°S–2°N, with values of 2.41, 1.2, 0.8, 0.6, and 0.48 m/s, for the first five baroclinic modes, respectively. The dispersion relation for Rossby waves is derived from $\omega_{RW} \approx -\frac{k}{k^2+2n+1}, (n \geq 1)$ (An et al., 2021).

dominate deeper layers of 400–800 m, representing a total averaged contribution approximately of 52.10% (Figure 7c).

The velocity time series reconstructed from the first through fifth baroclinic modes demonstrate that the sum of these modes aligns well with the reconstruction from the first mode of the CEOF (Figures 8a and 8b). This alignment indicates that Kelvin wave propagation is the primary mechanism driving intraseasonal variability in the northern Makassar Strait. Specifically, the reconstructed time series of mode 1 show a decreasing amplitude with depth and capture intraseasonal variability in the upper 350 m, contributing approximately 41 ± 20% of the variance (Figures 8a–8c). Mode 2 generates out-of-phase intraseasonal variability between the upper and deeper layers, according to its zero-crossing point depth (Figures 7b and 8d), contributing 18 ± 12% and 7 ± 4% of the total variance in the upper 400 m and 500–800 m, respectively. The time series from mode 3 exhibit similar phase variability compared to mode 2 but with a shallower depth (~200 m) where vertical phase differences occur (Figure 8e), contributing 9 ± 5% and 37 ± 16% of the total variance in the upper 200 m and 350–800 m, respectively. The time series from modes 4 and 5 display a three-layered structure, with mode 4 contributing 0.08 ± 0.09% (upper 250 m), 10 ± 8% (250–600 m), and 0.6 ± 0.6% (600–800 m), and mode 5 contributing 2 ± 1.7% (upper 150 m), 4.5 ± 5% (150–500 m), and 6.2 ± 4% (500–800 m) (Figures 8f and 8g). By comparing these results with the CEOF reconstruction (Figures 8a and 8b), we observe that the intraseasonal variability in the upper 300 m is primarily induced by the first three baroclinic modes, accounting for a total variance contribution of approximately 65 ± 28%. In contrast, the second to fifth baroclinic modes contribute roughly 50 ± 36% of the variance for intraseasonal variability between 300 and 800 m, surpassing the contribution of mode 1. Notably,

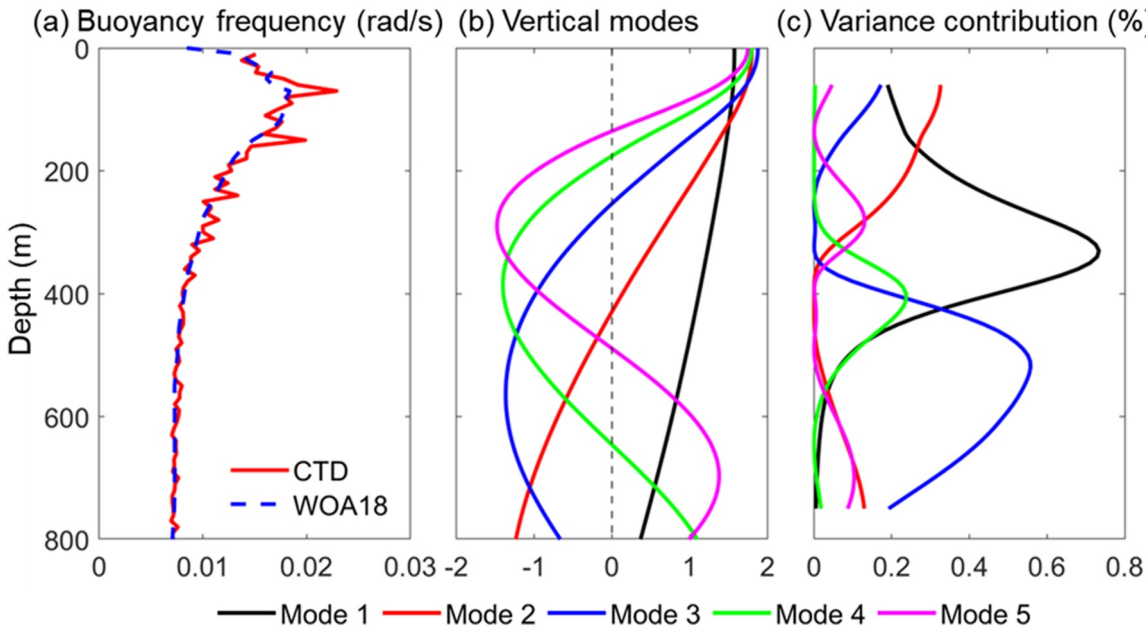

Figure 7. (a) Buoyancy frequency and the corresponding (b) vertical structures, and (c) variance contribution of the first five baroclinic Kelvin wave modes in the northern Makassar Strait (MakN: 0°57.09′N, 119°15.95′E).

modes 4 and 5 contribute 10.6 ± 8.6% (250–800 m) and 6.2 ± 4% (500–800 m) of the variance for intraseasonal variability, respectively. These findings underscore the significance of higher baroclinic modes for intraseasonal variability in the sub-thermocline, aligning with the ω-l diagram (Figure 6).

The intraseasonal zonal wind anomalies over the central equatorial Indian Ocean are identified as the driving force of the equatorial Kelvin waves, which propagate eastward and then southeastward/northwestward along the Sumatra–Java coasts as coastal Kelvin waves (Han, 2005; Iskandar et al., 2005; Schiller et al., 2010). Here, we calculate the lag correlations of sea surface zonal wind stress (τ_x) over the central equatorial Indian Ocean with current velocities (u' and/or v') in the mooring sites, that is, EQW, EQE, Lom, MakS, and MakN. Significant correlations occurred in the upper 150 m with lag time of around 0–15 days (peak at ∼5 days) at EQW and EQE (Figures 9a and 9b). In the Lombok Strait, significant correlations are lagged by 5–21 days (peak at ∼17 days) in the upper 260 m, with a vertical slope implying upward phase propagation (Figure 9c). The significant correlations move further northward to pass through the Makassar Strait, lagging by 12–30 days (MakS) and 15–45 days (MakN), respectively (Figures 9e and 9f). According to the lag correlation between τ_x and u' or v', the propagation phase speed is 2.17–3.08 m/s (from equatorial Indian Ocean to Lombok), 0.80–1.86 m/s (from Lombok to southern Makassar), and 0.34–1.01 m/s (from southern to northern Makassar), respectively.

To further elucidate the Kelvin wave signature in the northern Makassar Strait, we utilized a wind-forced Kelvin wave model by integrating τ_x along the characteristic $x–ct = constant$ pathway from the central equatorial Indian Ocean (70°E, 0°) to MakN, following the equator–coastal waveguide. The modeled velocities according to the first five baroclinic modes are shown in Figure 10. These modeled velocities align well with those reconstructed from the vertical mode decomposition (Figure 8), capturing the vertical structure and phase propagation of each mode, albeit with a slight offset of a few days (Figure 10). This suggests that wind-driven Kelvin waves propagate from the central equatorial Indian Ocean, along the Sumatra–Java coasts, penetrate the Indonesian seas through the Lombok Strait, and continue northward to the northern Makassar Strait across the equator.

3.5. Volume Transport Anomalies Associated With Kelvin Waves

Kelvin waves significantly impact the water transport by altering the velocity profile in the straits that ITF passes through. The Kelvin wave induced volume transport anomalies in the Lombok (Ombai) Strait were estimated as large as 0.8 ± 0.2 (2.1 ± 0.2) Sv, accounting for 34.78% (45.65%) of the annual mean transports, respectively (Drushka et al., 2010). Pujiana et al. (2013) suggested that the northward propagating Kelvin waves could reduce

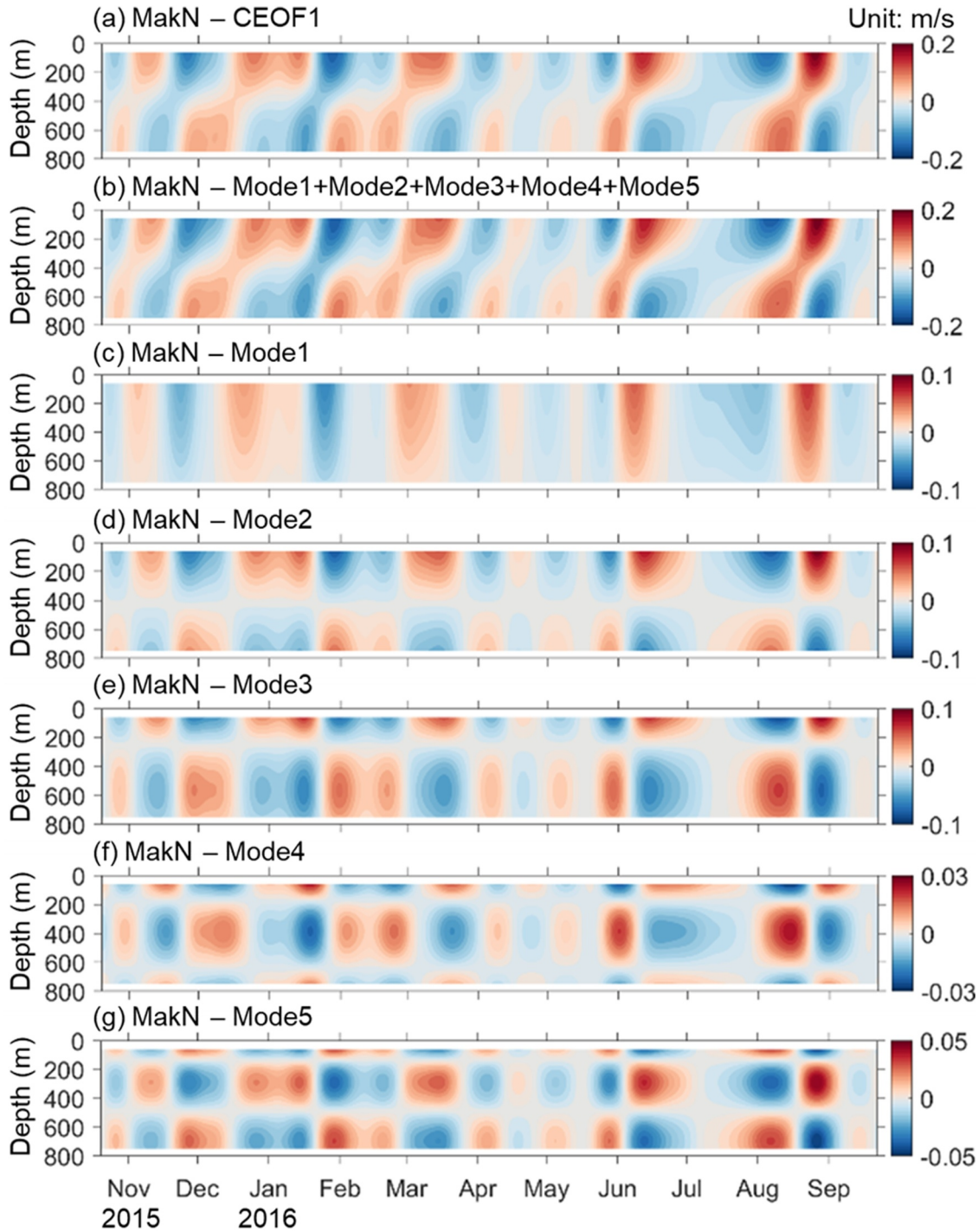

Figure 8. (a) Reconstructed intraseasonal current velocity anomaly based on the first CEOF mode (same as Figure 4e), (b) sum over first five baroclinic modes, and (c) the first, (d) second, (e) third, (f) fourth, and (g) fifth baroclinic modes in the northern of Makassar Strait (MakN: 0°57.09′N, 119°15.95′E).

the southward transport by up to 2 Sv within the pycnocline in the Makassar Strait. Based on MakN mooring, we estimated the total volume transport and its intraseasonal anomalies associated with Kelvin waves (Figure 11). The mean transport in the upper 800 m is 9.06 Sv during the observation period, with a standard deviation of 7.49 Sv, and intraseasonal standard deviation of 3.56 Sv. The first five Kelvin wave modes could explain a standard deviation of 1.89 Sv, accounting for 53.09% of the intraseasonal variability in the upper 800 m. To be specific, modes 1–2 dominate upper layer transport (0–400 m), accounting for 67.08% of the intraseasonal

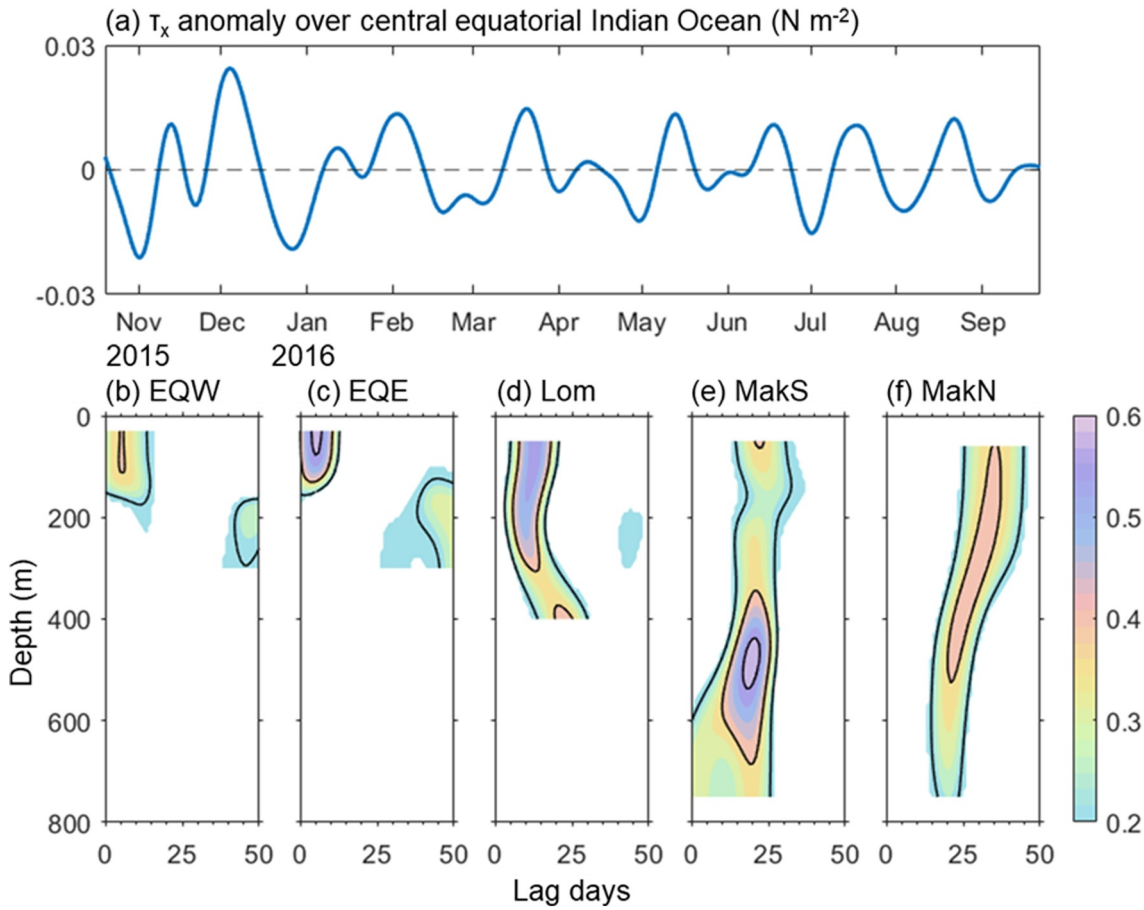

Figure 9. (a) Area averaged intraseasonal zonal wind stress (τ_x) over the central equatorial Indian Ocean (75°–90°E, 4°S–4°N) and its correlation with intraseasonal zonal velocity anomalies (u') in (b) EQW (0°, 80.5°E) and (c) EQE (0°, 90°E), and along strait velocity anomalies (v') in (d) Lombok Strait (Lom: 8°25.14′S, 115°57.59′E), (e) Southern Makassar Strait (MakS: 2°51.9′S, 118°27.3′E), and Northern Makassar Strait (MakN: 0°57.09′N, 119°15.95′E), with the later lagging by 0–50 days. Only correlation coefficients above the 95% significance level are plotted in (b–f).

variation; modes 3–5 dominate deeper layers transports, accounting for 49.07% (400–600 m) and 51.39% (600–800 m) of the intraseasonal variation, respectively.

4. Discussion and Conclusions

Previous studies have established the propagation of intraseasonal Kelvin waves from the central equatorial Indian Ocean to the Lombok Strait, predominantly in the first two baroclinic modes (e.g., Iskandar et al., 2006; Schiller et al., 2010). Once these waves penetrate the Lombok Strait, they continue their propagation as the second and third baroclinic modes along the 100-m isobath, reaching the southern Makassar Strait (Pujiana et al., 2013). This study advances our understanding by demonstrating that these Kelvin waves propagate northward across the equator and enter the northern Makassar Strait, potentially continuing further eastward along the north coast of Sulawesi Island (Figure 11). Notably, the dominant baroclinic modes shift during this propagation: from the first and second modes in the Indian Ocean, to the second and third modes between Lombok and southern Makassar, and finally to the third to fifth modes across the Makassar Strait. Additionally, the upward phase speed is faster in the Lombok Strait compared to that of the Indian Ocean and Makassar Strait. The mechanisms underlying these changes in dominant baroclinic modes and phase speed remain unresolved. However, considering the strong tidal mixing in the Lombok Strait (Ray & Susanto, 2016; Susanto et al., 2024) and substantial freshwater fluxes within the Indonesian seas (Kida et al., 2019; Lee et al., 2019; Xu et al., 2021), background stratification differences may contribute to these spatial variations. During the propagation, lower modes are more dissipated attributing to dramatic changes in stratification in the upper layer. In contrast, higher modes, which travel at a much deeper depth with less changes in stratification, tend to more conserved, thereby becoming increasingly dominant.

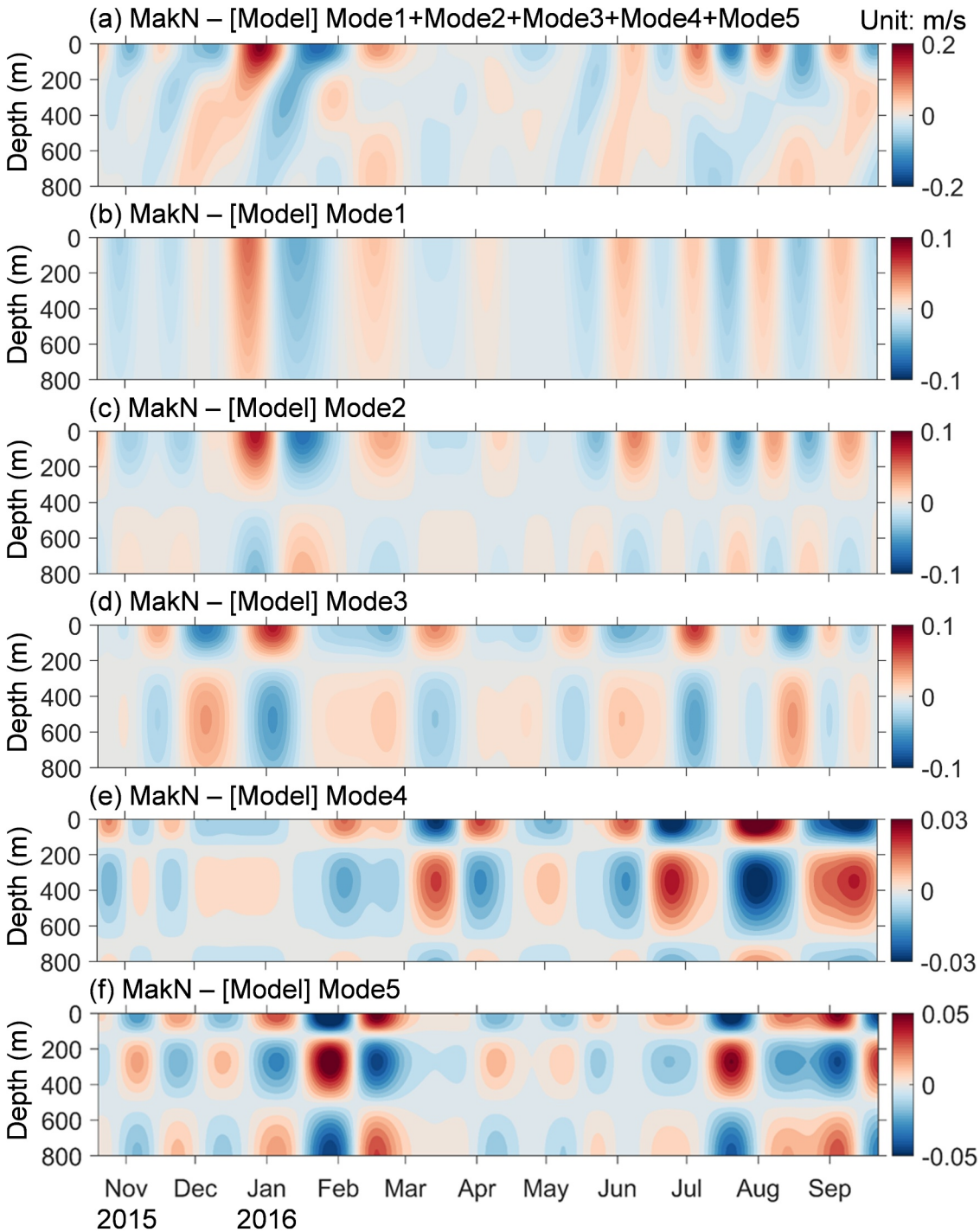

Figure 10. (a) Sum over first five modes of the wind forcing model, and modeled (b) mode 1, (c) mode 2, (d) mode 3, (e) mode 4, and (f) mode 5 in the northern Makassar Strait (MakN: 0°57.09′N, 119°15.95′E). The model was forced with winds along the waveguide of the Kelvin waves as shown by shaded region in Figure 1.

Consequently, the lower modes (modes 1 and 2) and higher modes (modes 3–5) tend to induce transport anomaly in the upper 400 m and 400–800 m, respectively.

It should be possible for the Kelvin waves to propagate further into the Sulawesi Sea after arriving at MakN. This is reflected in the theoretical model results by Yuan et al. (2018), and by albeit weak evidence from satellite altimeter data (Figures 1 and 2). If we roughly estimate the *KE* of the first five baroclinic modes based on moored

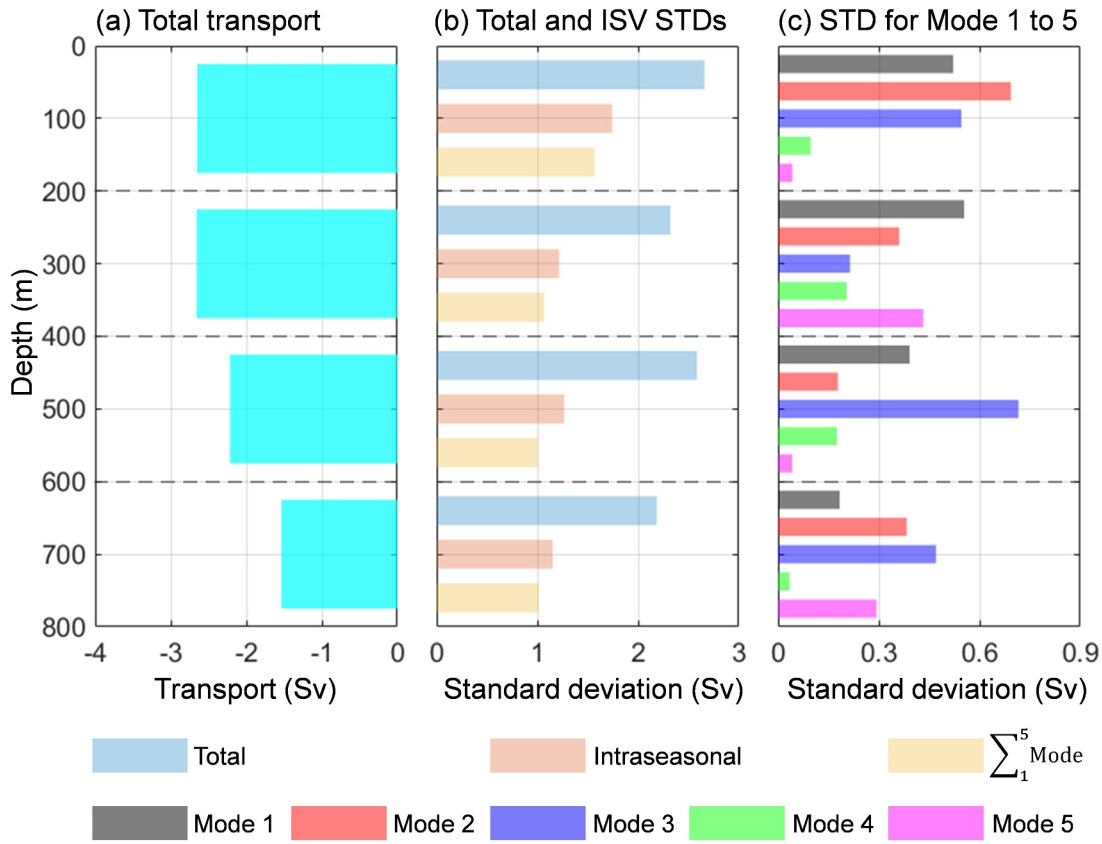

Figure 11. (a) Annual mean volume transport in different depth layers based on mooring-observed velocity in the northern Makassar Strait (MakN: 0°57.09′N, 119° 15.95′E); (b) standard deviations of the volume transport, the intraseasonal transport anomalies (20–90 days bandpass filtered), and those derived from the sum of the first five baroclinic modes; (c) standard deviation of the volume transport anomalies derived from each of the first five baroclinic modes.

velocities, there is 58% Kelvin wave energy penetrating into the Indonesian seas through the Lombok Strait, which is in agreement with previous investigations (Drushka et al., 2010; Syamsudin et al., 2004). Then, 22% of the *KE* from Lombok is found in MakN, roughly equivalent to 12% of the Kelvin waves from the Indian Ocean, which is corroborated by the theoretical model of Yuan et al. (2018). Therefore, it is expected that the Kelvin wave could travel further into the Sulawesi Sea; however, the wave energy would decay to less than 10% of its initial state.

Besides the Kelvin wave signal, a southward propagation from the northern to southern Makassar Strait is also identified by the ω–l relationship (Figure 6). However, the observed scatter points do not align well with the theoretical solution for Rossby waves. Previous research studies have suggested an intraseasonal frequency band centered around 50 days and/or eddy shedding from the Mindanao Current in the Sulawesi Sea, with a life cycle of 40–50 days (Chen et al., 2018; Hao et al., 2022; Masumoto et al., 2001; Qiu et al., 1999). One plausible source of this southward propagating signal is intraseasonal variability in the Sulawesi Sea, as proposed by Pujiana et al. (2009), who found coherent fluctuations between intraseasonal SLA in the Sulawesi Sea and intraseasonal velocity anomalies in the southern Makassar Strait. Alternatively, this signal could be attributed to coastal Kelvin waves that propagate along the 100-m isobath from the Makassar Strait, are captured by the equator, and then propagate eastward along the equator within the Makassar Strait. Upon reaching the Sulawesi coast, these Kelvin waves propagate northward towards the northern Makassar Strait. According to Kelvin wave dynamics, the abovementioned Kelvin waves may also propagate southward along the Sulawesi coast. This process, however, is difficult to identify because of its complicated interactions with the incident Kelvin waves from Lombok Strait. Nevertheless, given that the Rossby deformation radius (≈100 km) is smaller than the width of the Makassar Strait (130–250 km), the hypothesis of Kelvin wave propagation may help explain the observed northward/southward propagating signal. The pathways of the Kelvin waves are schematically shown in Figure 12. It should be noted

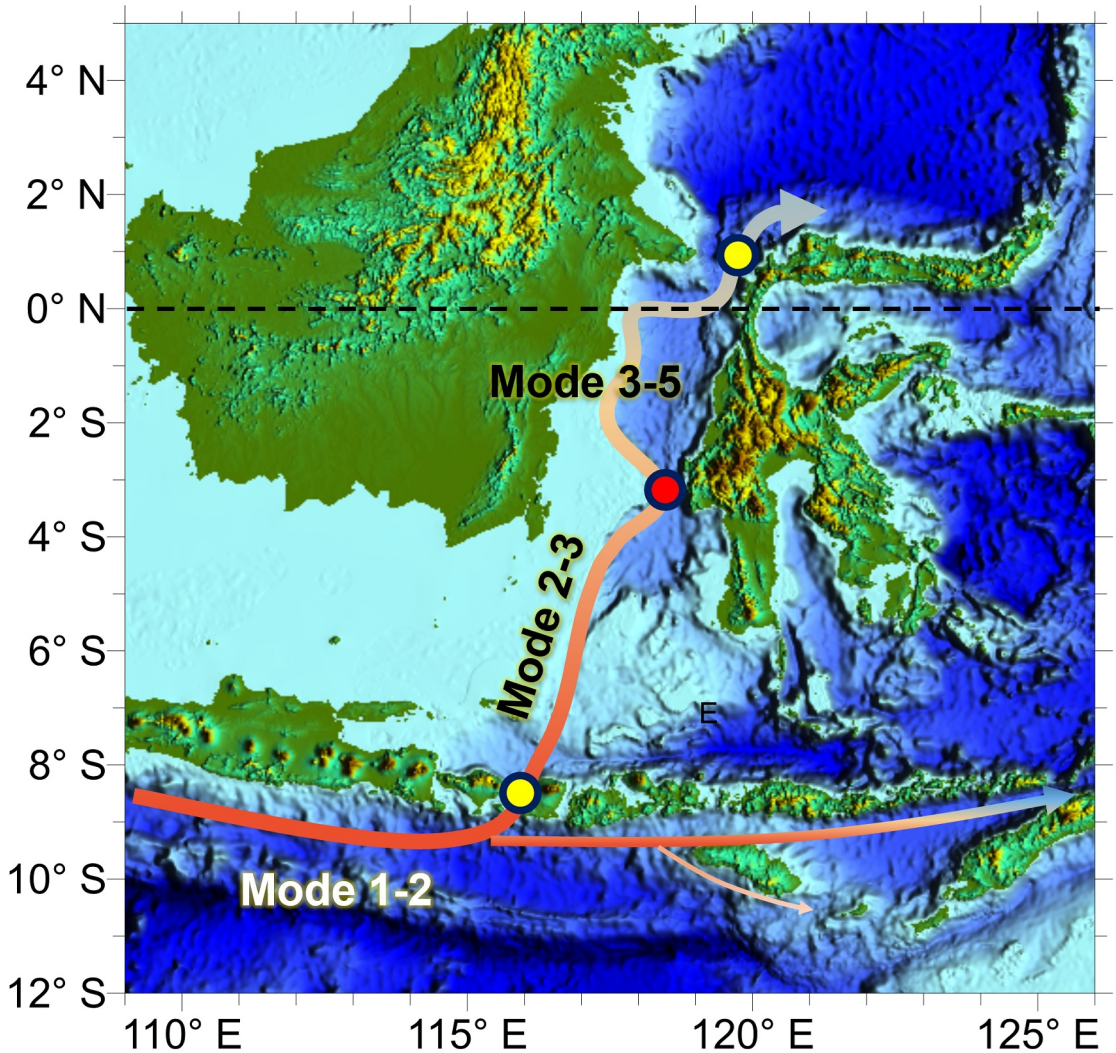

Figure 12. Schematic map of the Kelvin waves propagation in the Indonesian seas. Solid curve arrows indicate the waveguides for the Kelvin waves.

that the precise dynamics and quantitative decoupling of signals from Sulawesi and the Indian Ocean in the Makassar Strait require further investigation.

Vertical propagation of Kelvin waves has been identified as a key mechanism influencing the variability of the Indian Ocean equatorial intermediate current (Huang et al., 2018) and the middle layer current in the Savu Strait (Wang et al., 2020), with typical depths of 200–1,000 m and 280–800 m, respectively. This study extends this understanding by noting that Kelvin wave propagation also governs the along-strait flow in the sub-thermocline of the Makassar Strait. The ITF exhibits a subsurface velocity maximum (V-max) in the Makassar Strait, attributed to a surface freshwater plug (Gordon et al., 2019). Seasonal variability in V-max is associated with the seasonally reversed Karimata Throughflow, which transports significant freshwater from the South China Sea (SCS) to form the freshwater plug during boreal winter (Gordon et al., 2019; Jiang et al., 2019; Xu et al., 2021). Interannual variability in V-max is linked to the El Niño-Southern Oscillation (ENSO), which modulates both precipitation over the Indonesian seas and inflow from the SCS via the Mindoro–Sibutu passage (Jiang et al., 2019; Li et al., 2019). On the intraseasonal timescale, vertically propagating Kelvin waves are likely to have a significant impact on V-max, both in terms of depth and magnitude, warranting further investigation.

In conclusion, our findings highlight the complex and dynamic nature of Kelvin wave propagation in the Indonesian and Indian Ocean regions, with shifting dominant baroclinic modes and phase speeds. Additionally, the study introduces new insights into the sources and behavior of southward propagating signals in the Makassar

Strait. Future research studies should focus on elucidating the underlying mechanisms responsible for these observations and their implications for regional ocean dynamics and the Indonesian Throughflow.

5. Summary

The TIMIT project deployed moorings in Lombok and the northern Makassar Strait from 2013 to the present, with overlapping observations from 2015.10.20 to 2016.09.22 at a MITF mooring in the southern Makassar Strait. Utilizing these synchronous mooring data, we analyzed intraseasonal variability and its propagation across the equator from Lombok to the northern Makassar Strait. Results indicate significant intraseasonal amplitudes of 0.33, 0.25, and 0.33 m/s in the Lombok, northern, and southern Makassar Straits, respectively (Figures 3 and 4). CEOF and Vertical mode decomposition revealed that these intraseasonal flows are driven by the propagation of the first five baroclinic Kelvin waves. Intraseasonal zonal wind anomalies in the central equatorial Indian Ocean excite Kelvin waves, primarily in the first and second baroclinic modes, which propagate eastward. Upon encountering the eastern boundary, these waves transform into coastally trapped Kelvin waves and propagate southeastward and northwestward along the Sumatra–Java coasts. During southeastward propagation, coastal Kelvin waves penetrate the Indonesian seas through the Lombok Strait and continue northward to the Sulawesi Sea across the Makassar Strait. The dominant baroclinic modes shift from modes 1 and 2 in the Indian Ocean to modes 2 and 3 from Lombok to the southern Makassar Strait and to modes 3–5 from the southern to northern Makassar Strait. This alternation in dominant modes may be linked to complex background stratification influenced by strong tidal mixing.

Data Availability Statement

The AVISO SSH data are available at https://data.marine.copernicus.eu/product/SEALEVEL_GLO_PHY_L4_MY_008_047/files?subdataset=cmems_obs-sl_glo_phy-ssh_my_allsat-l4-duacs-0.125deg_P1D_202411. The CCMP wind data are available at https://data.remss.com/ccmp/v02.0. The bathymetry ETOPO1 data are available at https://www.ngdc.noaa.gov/thredds/catalog/global/ETOPO2022/60s/60s_geoid_netcdf/catalog.html?dataset=globalDatasetScan/ETOPO2022/60s/60s_geoid_netcdf/ETOPO_2022_v1_60s_N90W180_geoid.nc. The TIMIT observations are available at https://zenodo.org/records/14992370. We appreciate Gordon A.L. for sharing the MITF Makassar data that are available at https://academiccommons.columbia.edu/doi/10.7916/d8-p78a-zm51.

Acknowledgments
This study is jointly supported by the Laoshan Laboratory (LSKJ202202700), the Basic Scientific Fund for National Public Research Institutes of China (2024Q02), and the National Natural Science Foundation of China (42076023, 42430402, 42376034). RDS is supported by the Physical Oceanography program of the National Science Foundation (NSF; Grant 2242151) through the University of Maryland. We greatly appreciate the captain and the crews of Baruna Jaya VIII for their skillful operation during the voyages and their cooperation in the fieldwork, and we thank all participants in the TIMIT cruises.

References

An, S.-I., Wang, C., & Mechoso, C. (2021). Teleconnections in the atmosphere. *Interacting Climates of Ocean Basins*, 54–88. https://doi.org/10.1017/9781108610995.003

Arief, D., & Murray, S. P. (1996). Low-frequency fluctuations in the Indonesian Throughflow through Lombok Strait. *Journal of Geophysical Research*, *101*(C5), 12455–12464. https://doi.org/10.1029/96JC00051

Chen, G., Han, W., Li, Y., & Wang, D. (2016). Interannual variability of equatorial eastern Indian Ocean upwelling: Local versus remote forcing. *Journal of Physical Oceanography*, *46*(3), 789–807. https://doi.org/10.1175/JPO-D-15-0117.1

Chen, G., Han, W., Li, Y., Wang, D., & Shinoda, T. (2015). Intraseasonal variability of upwelling in the equatorial Eastern Indian Ocean. *Journal of Geophysical Research: Oceans*, *120*(11), 7598–7615. https://doi.org/10.1002/2015JC011223

Chen, X., Qiu, B., Chen, S., Cheng, X., & Qi, Y. (2018). Interannual modulations of the 50-day oscillations in the Celebes Sea: Dynamics and impact. *Journal of Geophysical Research: Oceans*, *123*(7), 4666–4679. https://doi.org/10.1029/2018JC013960

Drushka, K., Sprintall, J., Gille, S. T., & Brodjonegoro, I. (2010). Vertical structure of Kelvin waves in the Indonesian Throughflow exit passages. *Journal of Physical Oceanography*, *40*(9), 1965–1987. https://doi.org/10.1175/2010JPO4380.1

Durgadoo, J. V., Rühs, S., Biastoch, A., & Böning, C. W. B. (2017). Indian Ocean sources of Agulhas leakage. *Journal of Geophysical Research: Oceans*, *122*(4), 3481–3499. https://doi.org/10.1002/2016JC012676

Gill, A. E. (1982). Atmosphere-ocean dynamics. Retrieved from https://api.semanticscholar.org/CorpusID:116672531

Gordon, A. L. (1986). Interocean exchange of thermocline water. *Journal of Geophysical Research*, *91*(C4), 5037–5046. https://doi.org/10.1029/JC091iC04p05037

Gordon, A. L., & Fine, R. A. (1996). Pathways of water between the Pacific and Indian oceans in the Indonesian seas. *Nature*, *379*(6561), 146–149. https://doi.org/10.1038/379146a0

Gordon, A. L., Napitu, A., Huber, B. A., Gruenburg, L. K., Pujiana, K., Agustiadi, T., et al. (2019). Makassar strait Throughflow seasonal and interannual variability: An overview. *Journal of Geophysical Research: Oceans*, *124*(6), 3724–3736. https://doi.org/10.1029/2018JC014502

Gordon, A. L., Sprintall, J., Aken, H. M. V., Susanto, D., Wijffels, S., Molcard, R., et al. (2010). The Indonesian Throughflow during 2004–2006 as observed by the INSTANT program. *Dynamics of Atmospheres and Oceans*, *50*(2), 115–128. https://doi.org/10.1016/j.dynatmoce.2009.12.002

Han, W. (2005). Origins and dynamics of the 90-day and 30–60-day variations in the equatorial Indian Ocean. *Journal of Physical Oceanography*, *35*(5), 708–728. https://doi.org/10.1175/JPO2725.1

Hao, Z., Xu, Z., Feng, M., Zhang, P., & Yin, B. (2022). Dynamics of interannual eddy kinetic energy variability in the Sulawesi Sea revealed by OFAM3. *Journal of Geophysical Research: Oceans*, *127*(8), e2022JC018815. https://doi.org/10.1029/2022JC018815

Horii, T., Ueki, I., Syamsudin, F., Sofian, I., & Ando, K. (2016). Intraseasonal coastal upwelling signal along the southern coast of Java observed using Indonesian tidal station data. *Journal of Geophysical Research: Oceans*, *121*(4), 2690–2708. https://doi.org/10.1002/2015JC010886

Hu, X., Sprintall, J., Yuan, D., Tranchant, B., Gaspar, P., Koch-Larrouy, A., et al. (2019). Interannual variability of the Sulawesi Sea circulation forced by indo-pacific planetary waves. *Journal of Geophysical Research: Oceans*, *124*(3), 1616–1633. https://doi.org/10.1029/2018JC014356

Hu, X., Xue, H., & Liang, L. (2022). Impact of ENSO on the entrance of the Indonesian Throughflow: The oceanic wave propagation. *Journal of Geophysical Research: Oceans*, *127*(12), e2022JC018782. https://doi.org/10.1029/2022JC018782

Huang, K., Han, W., Wang, D., Wang, W., Xie, Q., Chen, J., & Chen, G. (2018). Features of the equatorial intermediate current associated with basin resonance in the Indian Ocean. *Journal of Physical Oceanography*, *48*(6), 1333–1347. https://doi.org/10.1175/JPO-D-17-0238.1

Iskandar, I., Mardiansyah, W., Masumoto, Y., & Yamagata, T. (2005). Intraseasonal Kelvin waves along the southern coast of Sumatra and Java. *Journal of Geophysical Research*, *110*(C4), C04013. https://doi.org/10.1029/2004JC002508

Iskandar, I., Masumoto, Y., Mizuno, K., Sasaki, H., Affandi, A. K., Setiabudidaya, D., & Syamsuddin, F. (2014). Coherent intraseasonal oceanic variations in the eastern equatorial Indian Ocean and in the Lombok and Ombai Straits from observations and a high-resolution OGCM. *Journal of Geophysical Research: Oceans*, *119*(2), 615–630. https://doi.org/10.1002/2013JC009592

Iskandar, I., & McPhaden, M. J. (2011). Dynamics of wind-forced intraseasonal zonal current variations in the equatorial Indian Ocean. *Journal of Geophysical Research*, *116*(C6), C06019. https://doi.org/10.1029/2010JC006864

Iskandar, I., Tozuka, T., Sasaki, H., Masumoto, Y., & Yamagata, T. (2006). Intraseasonal variations of surface and subsurface currents off Java as simulated in a high-resolution ocean general circulation model. *Journal of Geophysical Research*, *111*(C12), C12015. https://doi.org/10.1029/2006JC003486

Jiang, G. Q., Wei, J., Malanotte-Rizzoli, P., Li, M., & Gordon, A. L. (2019). Seasonal and interannual variability of the subsurface velocity profile of the Indonesian Throughflow at Makassar Strait. *Journal of Geophysical Research: Oceans*, *124*(12), 9644–9657. https://doi.org/10.1029/2018JC014884

Kessler, W. S., McPhaden, M. J., & Weickmann, K. M. (1995). Forcing of intraseasonal Kelvin waves in the equatorial Pacific. *Journal of Geophysical Research*, *100*(C6), 10613–10631. https://doi.org/10.1029/95JC00382

Kida, S., Richards, K. J., & Sasaki, H. (2019). The fate of surface freshwater entering the Indonesian seas. *Journal of Geophysical Research: Oceans*, *124*(5), 3228–3245. https://doi.org/10.1029/2018JC014707

Lee, T., Fournier, S., Gordon, A. L., & Sprintall, J. (2019). Maritime Continent water cycle regulates low-latitude chokepoint of global ocean circulation. *Nature Communications*, *10*(1), 2103. https://doi.org/10.1038/s41467-019-10109-z

Li, M., Gordon, A. L., Wei, J., Gruenburg, L. K., & Jiang, G. (2018). Multi-decadal timeseries of the Indonesian Throughflow. *Dynamics of Atmospheres and Oceans*, *81*, 84–95. https://doi.org/10.1016/j.dynatmoce.2018.02.001

Li, M., Wei, J., Wang, D., Gordon, A. L., Yang, S., Malanotte-Rizzoli, P., & Jiang, G. (2019). Exploring the importance of the Mindoro-Sibutu pathway to the upper-layer circulation of the South China Sea and the Indonesian Throughflow. *Journal of Geophysical Research: Oceans*, *124*(7), 5054–5066. https://doi.org/10.1029/2018JC014910

Masumoto, Y., Kagimoto, T., Yoshida, M., Fukuda, M., Hirose, N., & Yamagata, T. (2001). Intraseasonal eddies in the Sulawesi Sea simulated in an ocean general circulation model. *Geophysical Research Letters*, *28*(8), 1631–1634. https://doi.org/10.1029/2000GL011835

McCreary, J. P., & Anderson, D. L. T. (1984). A simple model of El Niño and the Southern Oscillation. *Monthly Weather Review*, *112*(5), 934–946. https://doi.org/10.1175/1520-0493(1984)112<0934:ASMOEN>2.0.CO;2

McPhaden, M. J., Meyers, G., Ando, K., Masumoto, Y., Murty, V. S. N., Ravichandran, M., et al. (2009). RAMA: The research moored array for African–Asian–Australian monsoon analysis and prediction*. *Bulletin of the American Meteorological Society*, *90*(4), 459–480. https://doi.org/10.1175/2008BAMS2608.1

McPhaden, M. J., Wang, Y., & Ravichandran, M. (2015). Volume transports of the Wyrtki jets and their relationship to the Indian Ocean Dipole. *Journal of Geophysical Research: Oceans*, *120*(8), 5302–5317. https://doi.org/10.1002/2015JC010901

Pujiana, K., Gordon, A. L., Metzger, E. J., & Ffield, A. L. (2012). The Makassar Strait pycnocline variability at 20–40 days. *Dynamics of Atmospheres and Oceans*, *53–54*, 17–35. https://doi.org/10.1016/j.dynatmoce.2012.01.001

Pujiana, K., Gordon, A. L., & Sprintall, J. (2013). Intraseasonal Kelvin wave in Makassar Strait. *Journal of Geophysical Research: Oceans*, *118*(4), 2023–2034. https://doi.org/10.1002/jgrc.20069

Pujiana, K., Gordon, A. L., Sprintall, J., & Susanto, R. (2009). Intraseasonal variability in the Makassar Strait thermocline. *Journal of Marine Research - J MAR RES*, *67*(6), 757–777. https://doi.org/10.1357/002224009792006115

Pujiana, K., & McPhaden, M. J. (2020). Intraseasonal Kelvin waves in the equatorial Indian Ocean and their propagation into the Indonesian seas. *Journal of Geophysical Research: Oceans*, *125*(5), e2019JC015839. https://doi.org/10.1029/2019JC015839

Qiu, B., Mao, M., & Kashino, Y. (1999). Intraseasonal variability in the Indo–Pacific Throughflow and the regions surrounding the Indonesian seas. *Journal of Physical Oceanography*, *29*(7), 1599–1618. https://doi.org/10.1175/1520-0485(1999)029<1599:IVITIP>2.0.CO;2

Ray, R. D., & Susanto, R. D. (2016). Tidal mixing signatures in the Indonesian seas from high-resolution sea surface temperature data. *Geophysical Research Letters*, *43*(15), 8115–8123. https://doi.org/10.1002/2016GL069485

Romea, R. D., & Allen, J. S. (1983). On vertically propagating coastal Kelvin waves at low latitudes. *Journal of Physical Oceanography*, *13*(7), 1241–1254. https://doi.org/10.1175/1520-0485(1983)013<1241:ovpckw>2.0.co;2

Schiller, A., Wijffels, S. E., Sprintall, J., Molcard, R., & Oke, P. R. (2010). Pathways of intraseasonal variability in the Indonesian Throughflow region. *Dynamics of Atmospheres and Oceans*, *50*(2), 174–200. https://doi.org/10.1016/j.dynatmoce.2010.02.003

Sprintall, J., Gordon, A. L., Koch-Larrouy, A., Lee, T., Potemra, J. T., Pujiana, K., & Wijffels, S. E. (2014). The Indonesian seas and their role in the coupled ocean–climate system. *Nature Geoscience*, *7*(7), 487–492. https://doi.org/10.1038/ngeo2188

Sprintall, J., Wijffels, S. E., Molcard, R., & Jaya, I. (2009). Direct estimates of the Indonesian Throughflow entering the Indian Ocean: 2004-2006. *Journal of Geophysical Research*, *114*(C07). https://doi.org/10.1029/2008JC005257

Susanto, R. D., Wei, Z., Santoso, P. D., Wang, G., Fadli, M., Li, S., et al. (2024). Field measurements of turbulent mixing south of the Lombok Strait, Indonesia. *Geoscience Letters*, *11*(1), 36. https://doi.org/10.1186/s40562-024-00349-3

Syamsudin, F., Kaneko, A., & Haidvogel, D. B. (2004). Numerical and observational estimates of Indian Ocean Kelvin wave intrusion into Lombok Strait. *Geophysical Research Letters*, *31*(24), L24307. https://doi.org/10.1029/2004GL021227

Terada, Y., & Masumoto, Y. (2023). Energy transmission pathways of equatorial waves within the Maritime Continent: A view with the wave energy flux. *Journal of Oceanography*, *79*(5), 517–536. https://doi.org/10.1007/s10872-023-00695-4

Tillinger, D., & Gordon, A. L. (2010). Transport weighted temperature and internal energy transport of the Indonesian Throughflow. *Dynamics of Atmospheres and Oceans*, *50*(2), 224–232. https://doi.org/10.1016/j.dynatmoce.2010.01.002

Wang, J., Yuan, D., Li, X., Li, Y., Wang, Z., Hu, X., et al. (2020). Moored observations of the Savu Strait currents in the Indonesian seas. *Journal of Geophysical Research: Oceans*, *125*(7), e2020JC016082. https://doi.org/10.1029/2020JC016082

Wei, Z., Li, S., Susanto, R. D., Wang, Y., Fan, B., Xu, T., et al. (2019). An overview of 10-year observation of the South China Sea branch of the Pacific to Indian Ocean Throughflow at the Karimata Strait. *Acta Oceanologica Sinica*, *38*(4), 1–11. https://doi.org/10.1007/s13131-019-1410-x

Wijffels, S., & Meyers, G. (2004). An intersection of oceanic waveguides: Variability in the Indonesian Throughflow region. *Journal of Physical Oceanography*, *34*(5), 1232–1253. https://doi.org/10.1175/1520-0485(2004)034<1232:AIOOWV>2.0.CO;2

Wyrtki, K. (1961). Physical oceanography of the south-east Asian waters. In *NAGA Report Vol. 2, Scientific Results of Marine Investigations of the South China Sea and the Gulf of Thailand* (p. 195). Scripps Institution of Oceanography. Retrieved from https://api.semanticscholar.org/CorpusID:130695237

Xie, T. X., Newton, R., Schlosser, P., Du, C. J., & Dai, M. H. (2019). Long-term mean mass, heat and nutrient flux through the Indonesian Seas, based on the tritium inventory in the Pacific and Indian Oceans. *Journal of Geophysical Research: Oceans*, *124*(6), 3859–3875. https://doi.org/10.1029/2018jc014863

Xu, T., Li, S., Hamzah, F., Setiawan, A., Susanto, R. D., Cao, G., & Wei, Z. (2018). Intraseasonal flow and its impact on the chlorophyll-a concentration in the Sunda Strait and its vicinity. *Deep Sea Research Part I: Oceanographic Research Papers*, *136*, 84–90. https://doi.org/10.1016/j.dsr.2018.04.003

Xu, T., Wei, Z., Cao, G., & Li, S. (2016). Pathways of intraseasonal Kelvin waves in the Indonesian Throughflow regions derived from satellite altimeter observation. *Atmospheric and Oceanic Science Letters*, *9*(5), 375–380. https://doi.org/10.1080/16742834.2016.1208047

Xu, T., Wei, Z., Susanto, R. D., Li, S., Wang, Y., Wang, Y., et al. (2021). Observed water exchange between the South China Sea and Java Sea through Karimata Strait. *Journal of Geophysical Research: Oceans*, *126*(2), e2020JC016608. https://doi.org/10.1029/2020JC016608

Xu, T., Wei, Z., Zhao, H., Guan, S., Li, S., Wang, G., et al. (2024). Simulated Indonesian Throughflow in Makassar Strait across the SODA3 products. *Acta Oceanologica Sinica*, *43*(1), 80–98. https://doi.org/10.1007/s13131-023-2186-6

Yuan, D., Hu, X., Xu, P., Zhao, X., Masumoto, Y., & Han, W. (2018). The IOD-ENSO precursory teleconnection over the tropical Indo-Pacific Ocean: Dynamics and long-term trends under global warming. *Journal of Oceanology and Limnology*, *36*(1), 4–19. https://doi.org/10.1007/s00343-018-6252-4

Zhang, T. C., Wang, W. Q., Xie, Q., & Chen, L. F. (2019). Heat contribution of the Indonesian Throughflow to the Indian Ocean. *Acta Oceanologica Sinica*, *38*(4), 72–79. https://doi.org/10.1007/s13131-019-1414-6